Central European Geology, Vol. 54/3, pp. 271–294 (2011)
DOI: 10.1556/CEuGeol.54.2011.3.5

Metallogenic implications of biotite chemical composition: Sample from Cu-Mo-Au mineralized granitoids of the Shah Jahan Batholith, NW Iran

Leila Zakeri, Farhad Malek-Ghasemi,
Ahmad Jahangiri, Mohssen Moazzen
Department of Geology, University of Tabriz, Tabriz

Igneous biotite has been analyzed from three I-type calc-alkaline intrusives of the Shah Jahan Batholith in NW Iran, which host several Cu-Mo-Au prospects. The X_{Mg} (Mg/Mg+Fe) value of biotite is the most significant chemical factor and the relatively high value of X_{Mg} corresponds to relatively high oxidation states of magma (estimated f_{O2} is mostly $10^{-12.5}$ to $10^{-7.5}$ bars), which is in good agreement with their host intrusions' setting and related ore occurrences. Based on criteria of Al^{IV} and Al^{VI} values, all studied biotites are primary ($Al^{VI} = 0$), and based on Al_{total} values (2.23–2.82 apfu) are in distinctive ranges of mineralized granitoid (Al_{total}=3.2 apfu).

The maximum F content of biotite from the Shah Jahan intrusions is moderately higher than those from some other calc-alkaline intrusions related to Cu-Mo porphyries in the world, and in contrast, Cl content is relatively lower. It is likely a result of primary magmatic vs. secondary hydrothermal origin, as well as the Mg-rich characteristics of the biotite in Shah Jahan. X_{Mg} values do not correlate with F and Cl contents of biotite, suggesting that biotite records changes in the F/OH and Cl/OH ratios in coexisting melt/fluids. It is consistent with F-compatible and Cl-incompatible behavior during fractional crystallization of wet calc-alkaline I-type granitoid magma generated at subduction related arc settings.

The fugacity ratios of (H_2O/HF), (H_2O/HCl) and (HF/HCl) magmatic solutions coexisting with biotite illustrate similar trends in the three intrusions, which can be due to parental magma sources and/or indicate occurrence of similar magmatic processes prior to or contemporaneous with exsolution of fluids from melt. The observed trends caused F-depletions and Cl-enrichments within developed magmatic-hydrothermal systems which are one of the essential characteristics of potential Cu-Mo-Au mineralized I-type granitoids.

Key words: biotite composition, Cu-Mo-Au mineralization, F-Cl fugacity ratios, f_{O2}; granitoid metallogeny

Addresses: L. Zakeri, F. Malek-Ghasemi, A. Jahangiri, M. Moazzen: 51664 Tabriz, Iran
e-mail: zakeri@tabrizu.ac.ir
Received: March 3, 2011; accepted: August 15, 2011

Introduction

The significance of micas for metallogenic studies resulted from their widespread occurrences in magmatic, metamorphic and hydrothermal ore-related environments, and in their application to estimating essential and intensive parameters such as the fugacity of O_2, H_2O, HCl and HF in coexisting melt/hydrothermal solutions (Munoz 1984, 1990, 1992; Zhu and Sverjensky 1991, 1992; Abdel-Rahman 1994; Selby and Nesbitt 2000; Nachit et al. 1985, 2005). The major part of these studies has focused on halogen contents of biotite in the felsic intrusions associated with deposits such as porphyry and skarn copper, molybdenum and gold deposits, with the objective of either distinguishing between mineralized and barren plutons, or linking characteristics of magmatic and associated mineralization systems (Wones and Eugster 1965; Beane 1974; Parry and Jacobs 1975; Jacobs and Parry 1979; Munoz and Swenson 1981; van Middelaar and Keith 1990; Loferski and Ayuso 1995; Aksyuk 2000; Lentz and Suzuki 2000; Sallet 2000; Coulson et al. 2001).

On the other hand, mineral chemistry of biotite in equilibrium with quartz, K-feldspar and magnetite can be used to estimate the oxidation state of the parental magma (Wones and Eugster 1965; Wones 1972, 1989). The X_{Mg} values of biotite are sensitive to the degree of oxidation of the parental magma, and furthermore influence values of F and Cl in biotite. X_{Mg} can be used as a useful tool to recognize prospective mineralized and barren granitoids, combined with F-Cl contents of primary magmatic biotite.

This contribution represents the first full elemental chemical composition study of magmatic biotites from the Cu-Mo-Au mineralization host plutons in the Shah Jahan Batholith, NW Iran (Fig. 1). The oxide and halogen contents in biotite were determined from least-altered samples of three intrusions. X_{Mg} biotite in equilibrium with quartz, K-feldspar and magnetite are used to estimate the oxidation state of the parental magma. F and Cl values of biotite are used to calculate the (fH_2O/fHF), ($fH_2O/fHCl$) and ($fHF/fHCl$) ratios of magmatic fluids. The results are compared with fugacity ratios determined for fluids related to some other porphyry style Cu-Mo-Au ore deposits and their host intrusions.

General geology and petrography

The Qaradagh batholithic complex, which is locally called the Ordobad Batholith with an area exceeding 1500 km^2, crops out at both sides of the Arax river in NW Iran, and south of the Azerbaijan and Armenia Republics. The most important Iranian segment of this great batholith crops out in Shah Jahan Mountain, of approximately 350 km^2 area, at the extreme north of Eastern Azarbaijan province. Shah Jahan is the largest granitoid batholith in Arasbaran, the main Cu (±Mo, Au) metallogenic belt of NW Iran which is in the lower Cenozoic Albourz–Azarbaijan magmatic arc (Fig. 1). The study area is located in the interior of the Shah Jahan Batholith, approximately 25 to 35 km northwest of the HaftCheshme and Sungun Cu ± Mo porphyry mines, respectively.

The Shah Jahan granitoids are characterized as medium to high-K calc-alkaline, meta-aluminous and I-type, magnetite series that formed in a magmatic arc setting related to subduction of the Neotethys oceanic crust (Zakeri et al. 2010). This batholith complex is composed of several distinct intrusions including gabbro, diorite, quartz diorite, quartz monzonite, quartz monzodiorite, leuco-

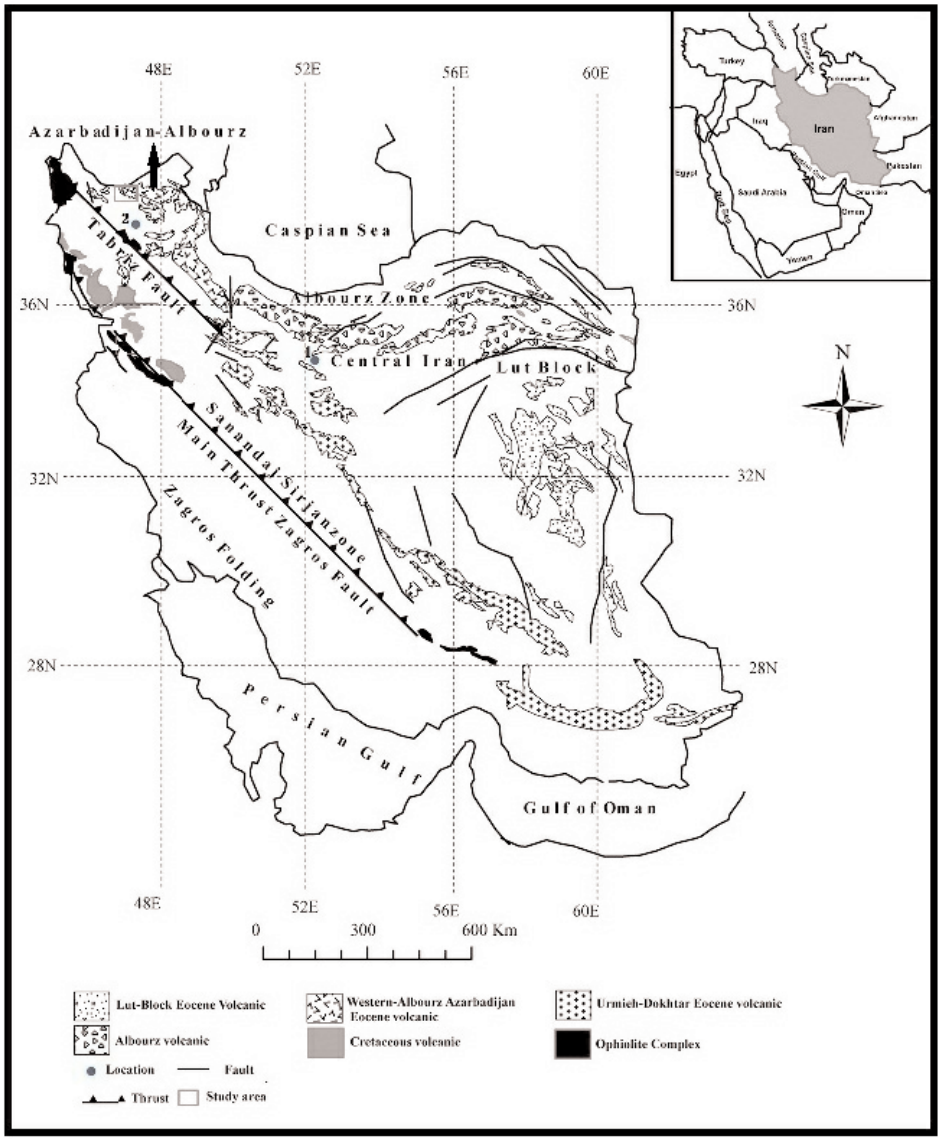

Fig. 1
Location map of the Shah Jahan batholith complex, south side of the northwest border of Iran (original tectonic map is from Alavi 1991)

tonalite, granodiorite, and monzogranite (Mokhtari 2009) in addition to some small stocks of quartz monzonite porphyry and a subvolcanic leuco-granite porphyry dome. Different parts of these plutons are commonly cross cut by dykes, commonly andesitic or rhyodacitic and occasionally aplitic. Some parts of the interior of this complex have diverse alterations, and various stock work to disseminated porphyry style mineralization and/or intrusion related quartz veins of Cu-Mo-Au (±Ag). The three sampled intrusions are the Garachilar Pluton and the Annigh Stock, and their country rock the Shah Jahan Pluton, which were sampled in the south of the Zarlidareh region (Fig. 2). The magmatic-hydrothermal activities occurring in various parts of the intrusions caused widely-scattered magmatic-hydrothermal alteration and concentrated Cu-Mo-Au±Ag mineralization in the Annigh, Zarlidareh and Garachilar regions.

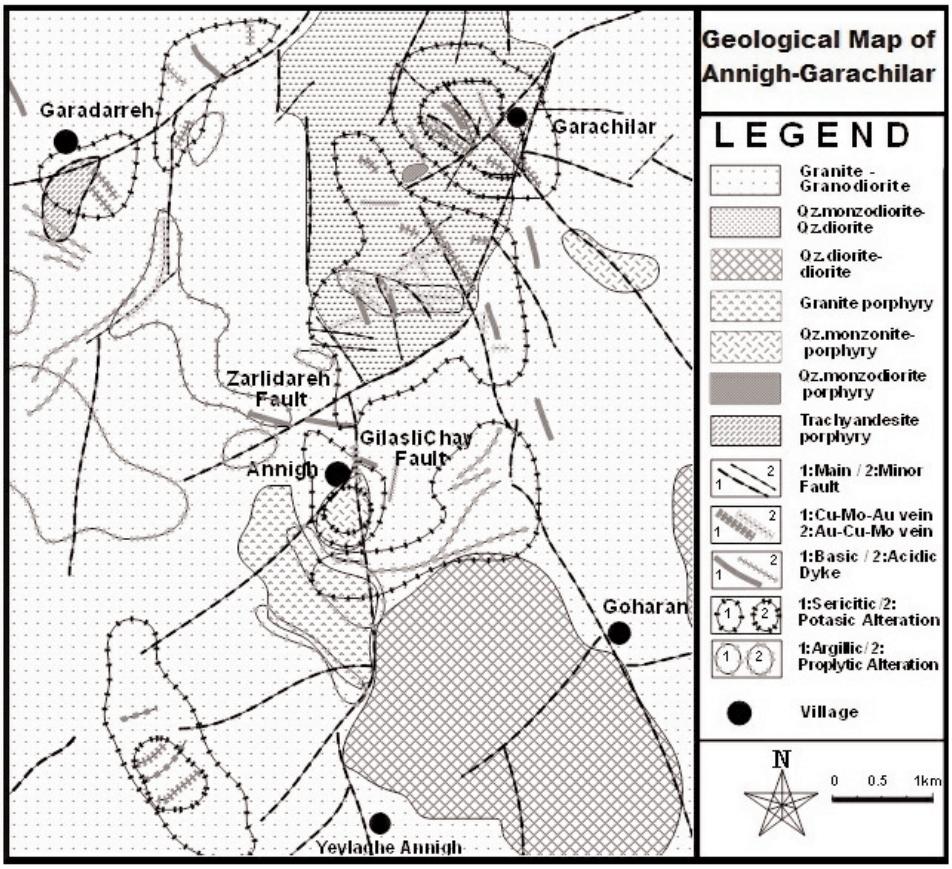

Fig. 2
Simplified geologic map of the studied area with locations of mineralized and altered zones of the Garachilar, Zarlidareh and Annigh areas, from the Shah Jahan Batholith

Although the three plutons are distributed over a large area, they show similar mineralogical paragenesis (Fig. 3). These calc-alkaline I-type granitoids commonly contain the magmatic assemblage of quartz + plagioclase + alkali-feldspar + biotite + hornblende and minor magnetite + titanite + apatite + zircon; alkali-feldspar, plagioclase and quartz considerably vary in proportion.

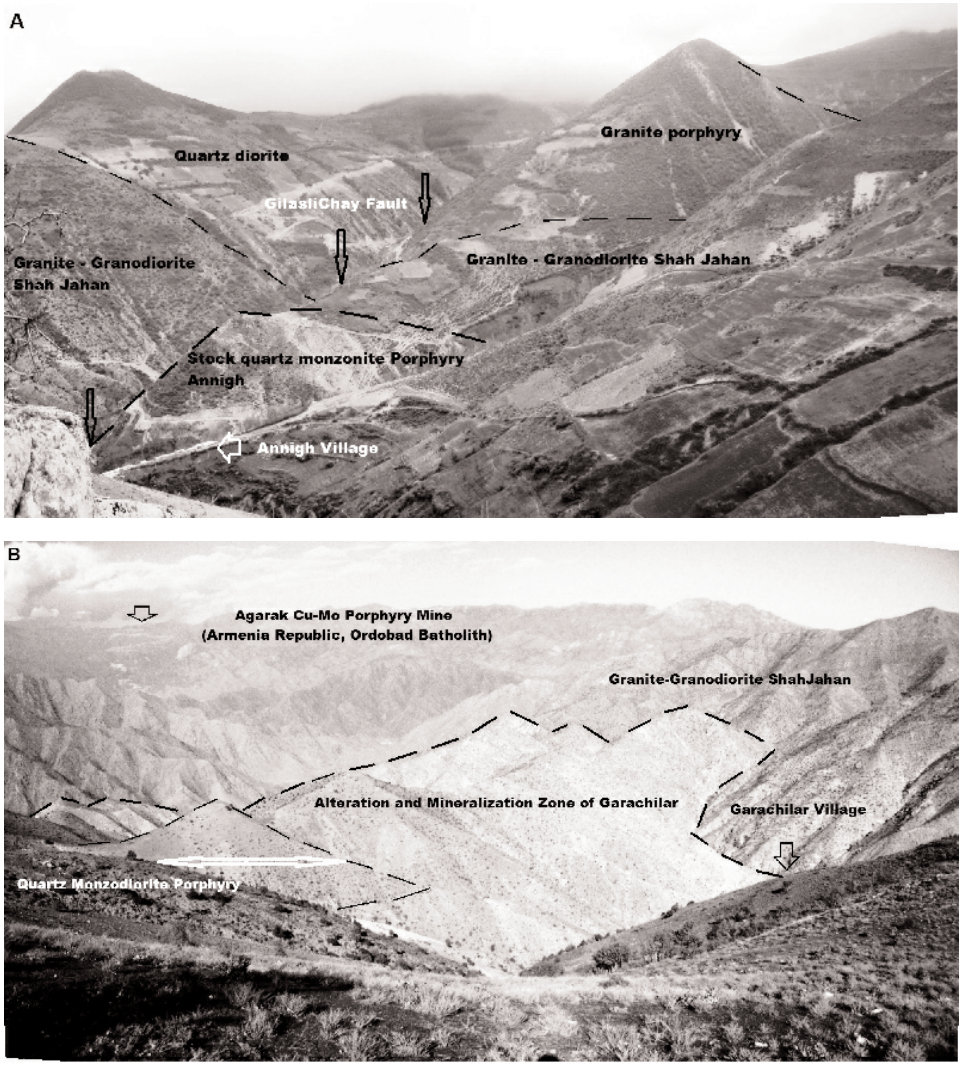

Fig. 3
Panoramic pictures of the study area. (A) View of the Annigh area from the north showing location of granite-granodiorite Shah Jahan, and the Annigh Stock with its alteration and mineralization prospect. (B) View of the Garachilar region from the south, showing the location of the Garachilar intrusion and its mineralization/alteration zone

Plagioclase forms subhedral to euhedral twinned grains and sometimes exhibits oscillatory zoning where the rim compositions are slightly more sodic. Alkali feldspar partly displays large microperthitic grains commonly containing small to moderate inclusions of euhedral to subhedral plagioclase with resorbed rims (Fig. 3A), and rarely myrmekite is present at the interface between plagioclase and adjacent K-feldspar grains. Hornblende and biotite are the only major ferromagnesian minerals and are frequently abundant (10–20%). Hornblende commonly is more abundant than biotite, except around the potassic alteration and mineralization zones. Part of the biotite and hornblende tend to occur together with euhedral to subhedral titanite (Fig. 3B) and magnetite as interstitial clots flanked by felsic minerals (Fig. 3). Apatite generally formed in the early stages of magma crystallization; therefore it can also be found, usually as inclusions in other minerals (Fig. 4B and F).

Shah Jahan Pluton

The dominant rock in the Shah Jahan Mountains (Figs 2 and 3) is a medium to rarely coarse-grained hornblende-biotite granodiorite to leuco-granite. It generally has subhedral equigranular texture (Fig. 4C and D), and grayish-white to pinkish-gray color. Late magmatic-hydrothermal alteration occurred and several mineralization zones were formed in Shah Jahan intrusive rocks, especially at their contact zones with some dykes and other intrusions, and in various faulted or brecciated zones. This pluton has a hornblende-biotite quartz monzodioritic composition in the Zarlidareh region (sampled zone) and contains several Au±Ag±Cu bearing quartz±carbonate veins (Fig. 2).

Garachilar Pluton

The Garachilar intrusion forms the north-northeastern part of the study area (Fig. 2) and is characteristically a medium- to fine grained hornblende-biotite quartz diorite to biotite-hornblende quartz monzodiorite, with inequigranular to equigranular texture (Fig. 4E and F). It is grayish-white to gray in color. In Garachilar, hydrothermal alteration and mineralization are principally present in

Fig. 4 →
Back-scattered electron images showing the mineral assemblage of the studied intrusions. (A) Annigh quartz monzonite with anhedral grains of alkali feldspar (Or.), which contains small to moderate inclusions of plagioclase (Pl.) showing the resorbed rims; (B) Annigh quartz monzonite; hornblende (Hbl.) occurs with euhedral to subhedral titanite (Ttn.) and magnetite (Mag.) between felsic minerals; apatite (Ap.) forms inclusions in the hornblende; (C) Quartz monzodiorite of Zarlidareh (Shah Jahan Pluton); hornblende occurs together with subhedral magnetite as a cluster between felsic minerals; (D) Quartz monzodiorite from Zarlidareh (Shah Jahan Pluton); hornblende includes anhedral secondary titanite and inclusions of magnetite; (E) Quartz diorite - quartz monzodiorite from the Garachilar Pluton containing large zoned plagioclase ,(F) Quartz diorite - quartz monzodiorite from the Garachilar Pluton containing titanite, ilmenite(Ilm) and euhedral apatites within magnetite as inclusions

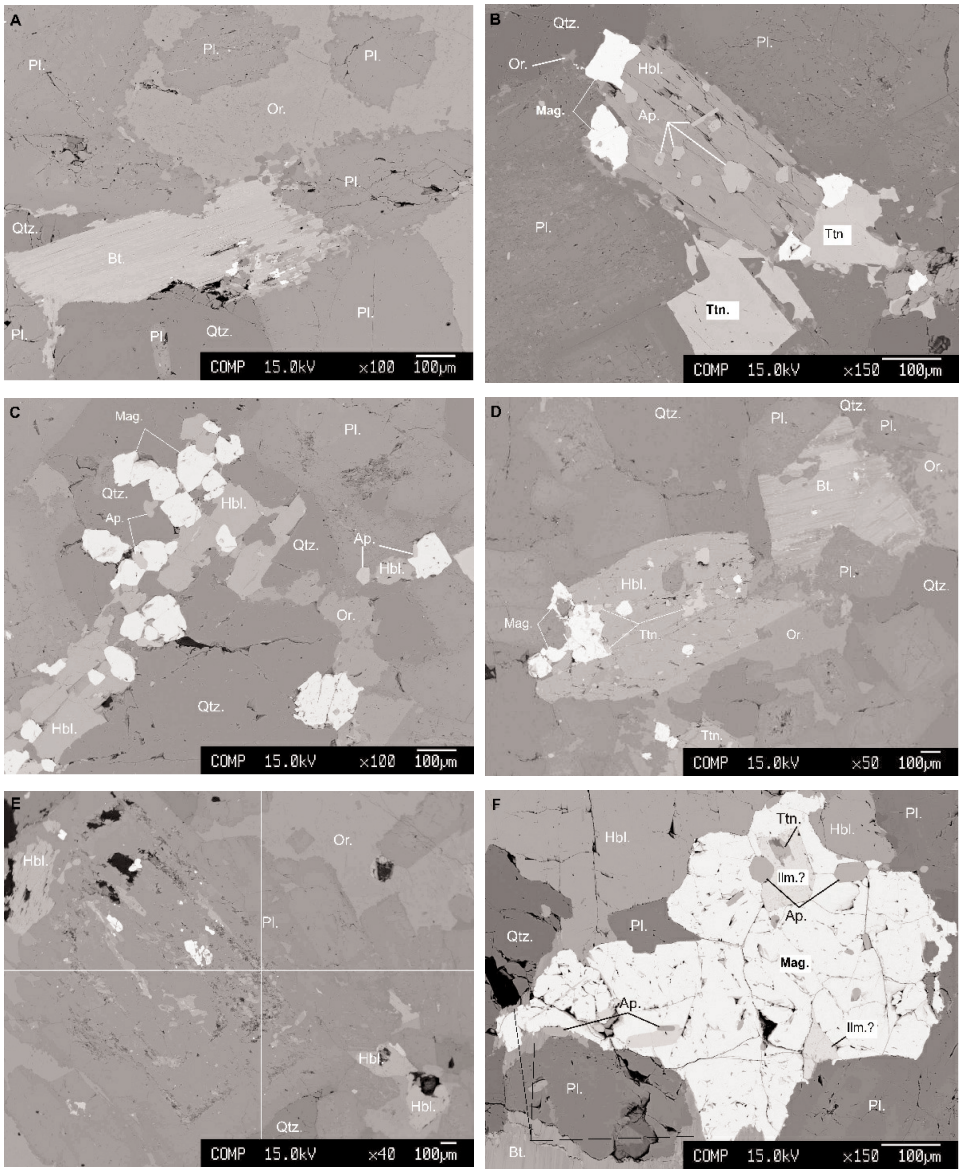

two sections of the intrusion. First, porphyry-style disseminated Cu-Mo mineralization in addition to several large quartz veins of Cu+Mo±Au occur in crushed regions west of Garachilar village, together with pervasive potassic and phyllic alteration (Fig. 3B). Second, adjacent to the Zarlidareh region there are Cu-Mo±Au±Ag-bearing hydrothermally brecciated quartz veins that are generally found with persistent phyllic alteration selvage.

Annigh stock

Annigh is a highly altered small stock situated between two major transverse faults. It is characteristically a medium to fine-grained hornblende-biotite quartz monzonite to granodiorite, with inequigranular and somewhere porphyric texture (Fig. 4A and B), and is grayish-white to greenish-white in color.

Stockwork-like pyrite-chalcopyrite-magnetite and molybdenite-bearing quartz veins and veinlets are scattered mainly in the northern and northwestern parts of this stock. Selectively pervasive potassic and intensive pervasive phyllic alteration zones irregularly occur in major parts of the Annigh intrusion, in addition to restricted late carbonate alteration zones. The highly destructive argillic alteration zones of both hypogene and supergene origins are typically associated with the late faults and intermittently overprinted phyllic and potassic alteration assemblages.

Types of biotite

In this study, biotite is divided into magmatic and secondary hydrothermal types (Fig. 5). Igneous biotite usually occurs as large to medium, euhedral to subhedral flakes (Fig. 5A). Altered igneous biotite is commonly observed in the late magmatic/or hydrothermal alteration assemblages and is partially or completely chloritized (Fig. 5D). Secondary biotite is inferred to be aggregates of fine-grained flecks of biotite precipitated from hydrothermal fluids responsible for potassic alteration. It occurs as either partial or complete replacements of magmatic biotite and hornblende (Fig. 5B), or was precipitated throughout the potassically altered rock (Fig. 5C) and in envelopes of quartz veins.

Studied samples were selected from the Garachilar and Annigh intrusives that contain mainly magmatic fresh biotite with rare chloritization at boundaries of some crystals. The Shah Jahan Pluton was sampled from a phyllic alteration zone within the Zarlidareh region (hearafter called Zarlidareh) that includes the least-altered and several partly chloritized magmatic biotite samples. Data from chloritized spots of biotites are not discussed here.

Methodology

All elemental analyses of biotites were obtained from polished thin sections using a JEOL JXA-8200 electron microprobe at the University of Leoben (Austria). Element determinations (Si, Al, Fe_{total}, Mg, Ti, Mn, Na, K, Ca, F and Cl) were carried out by EDS using a 1 μm beam, an accelerating potential voltage of 15 kV, a probe current of 10 nA, and a counting time of 20 s for each analysis. Natural biotite, amphibole, sanidine, tugtupite and willemite standards were used in the analytical procedure for F, Si, Al, Fe, Mg, Ti, Cl and Mn. Matrix effects were corrected using the ZAF software.

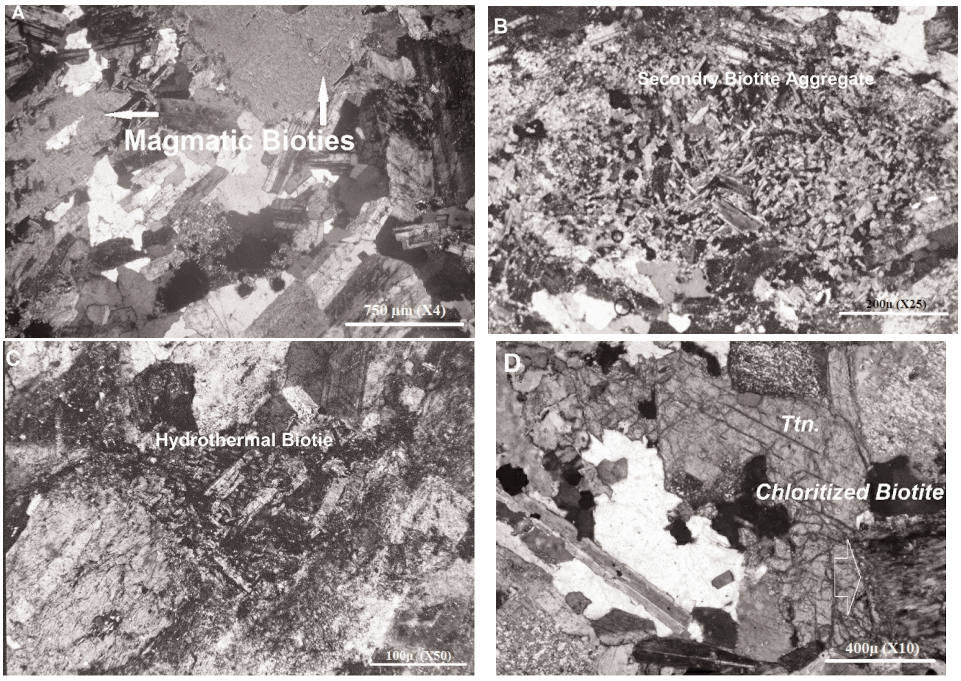

Fig. 5
Photomicrographs of biotite from the intrusions of the Shah Jahan area; (A) Large plates of early magmatic biotite from the Annigh Stock. (B) Intergrown aggregates of secondary hydrothermal biotite flakes that completely replaced early magmatic biotite/or hornblende, from potassic alteration zone of the Garachilar intrusion. (C) Fine-grained occurrences of hydrothermal biotite from the potassically altered Annigh Stock. (D) Altered magmatic biotite (chlorite replacing magmatic biotite) adjacent to a large euhedral titanite, from phyllic alteration zone of Zarlidareh

OH values were calculated on the basis of 22 oxygen formula units and assuming a total of 4 atoms in the hydroxyl site of biotite (ΣOH, F, Cl=4). The X_{Mg} and X_{Fe} values were determined from cation fractions and defined as Mg/(Mg+Fe) and Fe/(Fe+Mg+Al^{VI}), respectively (Zhu and Sverjensky 1992). X_{Cl}, X_F and X_{OH} are the mole fractions of Cl, F, and OH in the hydroxyl site.

Biotite major element chemistry

A total of 26 biotite grains were analyzed from the three intrusions of the Shah Jahan granitoidic complex (Table 1). Their compositions are graphically shown in Figs 6 and 7. As shown in a classification diagram (Fig. 6), and based on X_{Mg} phlogopite > 0.66 > X_{Mg} biotite (Deer et al. 1992; Rieder et al. 1998; Rieder 2001), biotite shows phlogopitic composition in Annigh and Zarlidareh, and biotitic composition with high Mg content in Garachilar samples (Zakeri et al. 2010).

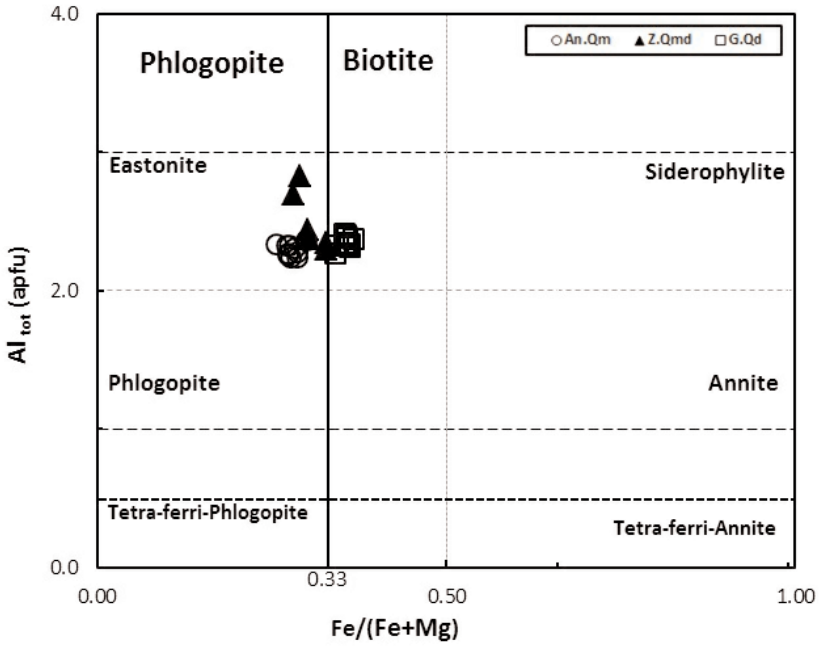

Fig. 6
Biotite classification based on X_{Fe} (here $X_{Mg}+ X_{Fe}=1$) vs. Al_{total} values for the three intrusions of the Shah Jahan granitoidic complex, the Annigh quartz monzonite (An.Qm), the Zarlidareh quartz monzodiorite (Z.Qmd), and the Garachilar quartz diorite (G.Qd)

X_{Mg} values of biotite (Fig. 7) are distributed in a restricted compositional field, and vary throughout the three rock types from 0.63 to 0.66, 0.67 to 0.72 and 0.70 to 0.74, which, respectively, correspond to Garachilar (G.Qd), Zarlidareh (Z.Qmd) and Annigh (An.Qm). It gradually increases with increasing acidity of the host rock, which is not in accordance with simple magmatic fractional crystallization (Deer et al. 1991).

Biotite from Garachilar is characterized by slightly higher FeO wt%, and lower MnO wt% (Fig. 7) than biotite from two other intrusions. Fe_{total} contents of biotite show a strong negative correlation with X_{Mg} and a weak negative correlation with Mn_{apfu} (atom per formula unit) values, suggesting Mg:Fe and/or Fe:Mn substitutions occurred. Maximum value of substitution observed in these samples for Mn:Fe is 0.1.

Tetrahedral sites of studied biotites are not completely filled with Si and Al_{total} ($\Sigma Si + Al_{total} < 8$ apfu, Table 1); therefore Ti can substitute at this site (Farmer and Boettcher 1981). Al_{total} is equal to Al^{IV}, and Al^{VI} content of these biotites is zero (Table 1). Nachit et al. (2005) reported that magmatic biotite commonly has low to zero content of Al^{VI}, whereas the re-equilibrated magmatic and hydrothermally neoformed biotite always has a high Al^{VI} content ($Al^{VI} > 1$ apfu. based on 22

Table 1
Composition of biotites* (wt.%) in studied samples of the Shah Jahan granitoids as determined by Electron Microprobe Analyses (EMPA)

Intrusion	Annigh Qm.										Zarlidareh Qmd.			
sample No.	bio-1	bio-2	bio-3	bio-4	bio-5	bio-6	bio-8	bio-9	bio-10	bio-11	bio-1	bio-2	bio-6	bio-7
(wt%)														
SiO_2	34.55	34.96	34.74	33.86	34.23	33.59	33.29	33.22	33.61	34.16	34.33	33.76	33.48	33.87
TiO_2	3.39	3.36	3.15	2.27	3.20	3.40	2.84	3.25	3.16	3.36	3.13	4.19	2.97	3.51
Al_2O_3	13.13	13.05	12.96	13.22	13.03	13.44	13.13	13.07	13.31	13.10	13.53	12.96	13.80	13.27
Cr_2O_3	0.02	0.00	0.02	0.00	0.00	0.01	0.01	0.00	0.00	0.00	0.00	0.02	0.00	0.01
FeO	15.90	16.26	15.88	14.83	15.66	16.29	15.42	15.88	15.69	15.65	16.40	17.17	16.45	17.44
MnO	0.54	0.55	0.74	0.55	0.60	0.55	0.54	0.64	0.63	0.56	0.61	0.69	0.60	0.65
MgO	22.34	22.78	23.26	24.21	23.30	21.45	23.26	22.74	23.17	23.31	21.20	19.85	21.45	20.09
CaO	0.03	0.01	0.04	0.17	0.03	0.09	0.11	0.02	0.00	0.01	0.04	0.05	0.02	0.09
Na_2O	0.03	0.10	0.08	0.11	0.06	0.12	0.05	0.09	0.07	0.11	0.11	0.07	0.10	0.07
K_2O	7.64	7.85	7.16	5.02	7.37	7.71	6.47	7.47	7.29	7.66	7.55	7.73	7.67	7.74
Cl	0.01	0.06	0.01	0.04	0.02	0.02	0.07	0.01	0.06	0.03	0.03	0.04	0.00	0.00
=O	0.00	-0.01	0.00	-0.01	0.00	0.00	-0.02	0.00	-0.01	-0.01	-0.01	-0.01	0.00	0.00
F	0.00	1.11	1.97	0.00	0.00	0.00	0.00	0.00	1.54	0.00	3.86	0.00	0.00	0.00
=O	0.00	-0.47	-0.83	0.00	0.00	0.00	0.00	0.00	-0.65	0.00	-1.63	0.00	0.00	0.00
Total	**97.59**	**99.60**	**99.18**	**94.27**	**97.50**	**96.65**	**95.16**	**96.40**	**97.87**	**97.94**	**99.16**	**96.51**	**96.55**	**96.73**
apfu(22 O_2)														
Si	5.08	5.09	5.08	5.06	5.04	5.01	5.00	4.97	4.98	5.01	5.10	5.07	5.01	5.07
Ti	0.37	0.37	0.35	0.26	0.35	0.38	0.32	0.37	0.35	0.37	0.35	0.47	0.33	0.40
Al	2.28	2.24	2.23	2.33	2.26	2.36	2.32	2.30	2.32	2.27	2.37	2.29	2.43	2.34
Cr	0.00	0.00	0.00	0.00	0.00	0.00	0.00	0.00	0.00	0.00	0.00	0.00	0.00	0.00
Fe tot	1.96	1.98	1.94	1.85	1.93	2.03	1.94	1.99	1.94	1.92	2.04	2.16	2.06	2.19
Mn	0.07	0.07	0.09	0.07	0.07	0.07	0.07	0.08	0.08	0.07	0.08	0.09	0.08	0.08
Mg	4.90	4.94	5.07	5.40	5.11	4.77	5.21	5.07	5.11	5.10	4.69	4.44	4.78	4.49
Ca	0.00	0.00	0.01	0.03	0.00	0.01	0.02	0.00	0.00	0.00	0.01	0.01	0.00	0.01
Na	0.01	0.03	0.02	0.03	0.02	0.03	0.02	0.03	0.02	0.03	0.03	0.02	0.03	0.02
K	1.43	1.46	1.34	0.96	1.38	1.47	1.24	1.42	1.38	1.43	1.43	1.48	1.46	1.48
Totals	**16.11**	**16.16**	**16.12**	**15.98**	**16.17**	**16.16**	**16.13**	**16.22**	**16.19**	**16.21**	**16.09**	**16.04**	**16.18**	**16.08**
OH	3.997	3.475	3.086	3.991	3.995	3.996	3.983	3.997	3.266	3.993	2.180	3.989	4.000	4.000
F	0.000	0.510	0.912	0.000	0.000	0.000	0.000	0.000	0.720	0.000	1.814	0.000	0.000	0.000
Cl	0.003	0.015	0.002	0.009	0.005	0.004	0.017	0.003	0.014	0.007	0.007	0.011	0.000	0.000
XOH	0.999	0.869	0.771	0.998	0.999	0.999	0.996	0.999	0.816	0.998	0.545	0.997	1.000	1.000
XF	0.000	0.128	0.228	0.000	0.000	0.000	0.000	0.000	0.180	0.000	0.453	0.000	0.000	0.000
XCl	0.001	0.004	0.001	0.002	0.001	0.001	0.004	0.001	0.004	0.002	0.002	0.003	0.000	0.000
Log XCl/XOH	-3.183	-2.362	-3.114	-2.636	-2.922	-2.962	-2.368	-3.137	-2.355	-2.762	-2.508	-2.570	0.000	0.000
Log XF/XOH	0.000	-0.833	-0.529	0.000	0.000	0.000	0.000	0.000	-0.657	0.000	-0.080	0.000	0.000	0.000
Log XF/XCl	0.000	1.528	2.585	0.000	0.000	0.000	0.000	0.000	1.698	0.000	2.428	0.000	∞	∞
log(fH_2O)/(fHF)	0.000	4.771	4.474	0.000	0.000	0.000	0.000	0.000	4.605	0.000	3.998	0.000	0.000	0.000
log(fH_2O)/($fHCl$)	5.402	4.581	5.336	4.871	5.148	5.174	4.595	5.358	4.579	4.988	4.717	4.766	0.000	0.000
log(fHF)/($fHCl$)	0.000	-0.608	0.437	0.000	0.000	0.000	0.000	0.000	-0.455	0.000	0.321	0.000	∞	∞
XFe	0.285	0.286	0.277	0.256	0.274	0.299	0.271	0.281	0.275	0.274	0.303	0.327	0.301	0.328
XMg	0.715	0.714	0.723	0.744	0.726	0.701	0.729	0.719	0.725	0.726	0.697	0.673	0.699	0.672
Si + Al	7.359	7.324	7.312	7.392	7.298	7.379	7.322	7.269	7.300	7.279	7.464	7.365	7.437	7.417
Al^{IV} = Al_{tot}	2.277	2.237	2.233	2.329	2.259	2.365	2.323	2.302	2.323	2.266	2.368	2.295	2.432	2.343
Si + Al + Ti	7.733	7.691	7.657	7.647	7.652	7.761	7.643	7.635	7.651	7.650	7.814	7.838	7.771	7.812

* Each column represents one point analysis per grain.

Table 1 (cont.)

Intrusion	Z.Qmd		Garachilar Qd.									
sample No.	bio-8	bio-10	bio-1	bio-2	bio-3	bio-4	bio-5	bio-6	bio-7	bio-8	bio-9	bio-11
(wt.%)												
SiO_2	31.70	27.95	33.82	34.19	33.78	33.64	33.87	33.49	33.27	33.86	33.18	33.50
TiO_2	1.22	0.67	3.72	4.03	3.80	3.91	4.10	3.81	4.15	3.56	4.09	5.38
Al_2O_3	14.90	15.53	13.22	13.02	13.38	13.06	13.06	13.31	12.95	13.53	13.06	12.76
Cr_2O_3	0.00	0.00	0.00	0.02	0.00	0.00	0.00	0.00	0.00	0.00	0.00	0.02
FeO	16.19	19.21	18.65	18.54	18.09	18.72	18.03	18.52	17.95	18.36	18.54	17.24
MnO	0.68	0.75	0.42	0.44	0.35	0.38	0.45	0.45	0.48	0.39	0.46	0.49
MgO	23.39	26.29	18.11	18.44	18.42	18.60	18.22	18.69	19.10	18.74	18.96	18.74
CaO	0.12	0.13	0.04	0.05	0.01	0.00	0.00	0.00	0.04	0.02	0.02	0.46
Na_2O	0.01	0.02	0.13	0.07	0.06	0.06	0.04	0.06	0.02	0.07	0.05	0.05
K_2O	4.18	3.32	7.88	7.80	7.72	7.84	8.06	8.19	7.73	7.87	8.10	7.85
Cl	0.02	0.03	0.02	0.01	0.04	0.03	0.07	0.02	0.03	0.02	0.07	0.01
=O	0.00	-0.01	0.00	0.00	-0.01	-0.01	-0.02	-0.01	-0.01	0.00	-0.02	0.00
F	0.00	1.04	1.53	3.85	0.00	0.00	0.00	0.00	1.54	3.43	4.26	0.00
=O	0.00	-0.44	-0.64	-1.62	0.00	0.00	0.00	0.00	-0.65	-1.44	-1.79	0.00
Total	**92.40**	**94.50**	**96.88**	**98.84**	**95.66**	**96.25**	**95.89**	**96.54**	**96.60**	**98.39**	**98.99**	**96.49**
apfu (22 O_2)												
Si	4.86	4.31	5.14	5.15	5.13	5.10	5.14	5.07	5.06	5.11	5.03	5.05
Ti	0.14	0.08	0.43	0.46	0.43	0.45	0.47	0.43	0.47	0.40	0.47	0.61
Al	2.69	2.82	2.37	2.31	2.40	2.34	2.34	2.38	2.32	2.41	2.33	2.26
Cr	0.00	0.00	0.00	0.00	0.00	0.00	0.00	0.00	0.00	0.00	0.00	0.00
Fe tot	2.08	2.48	2.37	2.34	2.30	2.37	2.29	2.34	2.28	2.32	2.35	2.17
Mn	0.09	0.10	0.05	0.06	0.05	0.05	0.06	0.06	0.06	0.05	0.06	0.06
Mg	5.35	6.04	4.10	4.14	4.17	4.21	4.13	4.22	4.33	4.22	4.29	4.21
Ca	0.02	0.02	0.01	0.01	0.00	0.00	0.00	0.00	0.01	0.00	0.00	0.07
Na	0.00	0.01	0.04	0.02	0.02	0.02	0.01	0.02	0.01	0.02	0.01	0.01
K	0.82	0.65	1.53	1.50	1.50	1.52	1.56	1.58	1.50	1.52	1.57	1.51
Totals	**16.05**	**16.51**	**16.03**	**15.99**	**15.99**	**16.05**	**16.00**	**16.10**	**16.04**	**16.04**	**16.12**	**15.96**
OH	3.995	3.486	3.261	2.159	3.989	3.993	3.982	3.994	3.253	2.359	1.938	3.999
F	0.000	0.507	0.735	1.837	0.000	0.000	0.000	0.000	0.739	1.635	2.044	0.000
Cl	0.005	0.007	0.004	0.004	0.011	0.007	0.018	0.006	0.008	0.006	0.019	0.001
XOH	0.999	0.871	0.815	0.540	0.997	0.998	0.995	0.998	0.813	0.590	0.484	1.000
XF	0.000	0.127	0.184	0.459	0.000	0.000	0.000	0.000	0.185	0.409	0.511	0.000
XCl	0.001	0.002	0.001	0.001	0.003	0.002	0.005	0.002	0.002	0.001	0.005	0.000
Log XCl/XOH	-2.882	-2.696	-2.916	-2.768	-2.546	-2.732	-2.344	-2.813	-2.628	-2.621	-2.014	-3.435
Log XF/XOH	0.000	-0.837	-0.647	-0.070	0.000	0.000	0.000	0.000	-0.644	-0.159	0.023	0.000
Log XF/XCl	0.000	1.858	2.269	2.698	0.000	0.000	0.000	0.000	1.984	2.461	2.037	0.000
log($fH2o$)/(fHF)	0.000	4.769	4.498	3.927	0.000	0.000	0.000	0.000	4.517	4.024	3.841	0.000
log($fH2o$)/($fHCl$)	5.104	4.911	5.092	4.947	4.728	4.911	4.525	4.993	4.814	4.803	4.196	5.624
log(fHF)/($fHCl$)	0.000	-0.269	0.262	0.682	0.000	0.000	0.000	0.000	-0.056	0.435	0.011	0.000
XFe	0.280	0.291	0.366	0.361	0.355	0.361	0.357	0.357	0.345	0.355	0.354	0.340
XMg	0.720	0.709	0.634	0.639	0.645	0.639	0.643	0.643	0.655	0.645	0.646	0.660
Si + Al	7.556	7.133	7.507	7.467	7.525	7.438	7.481	7.445	7.382	7.516	7.368	7.311
$Al^{IV} = Al_{tot}$	2.693	2.823	2.367	2.314	2.395	2.335	2.337	2.375	2.321	2.406	2.334	2.265
Si + Al + Ti	7.697	7.211	7.932	7.924	7.960	7.885	7.949	7.879	7.856	7.920	7.834	7.920

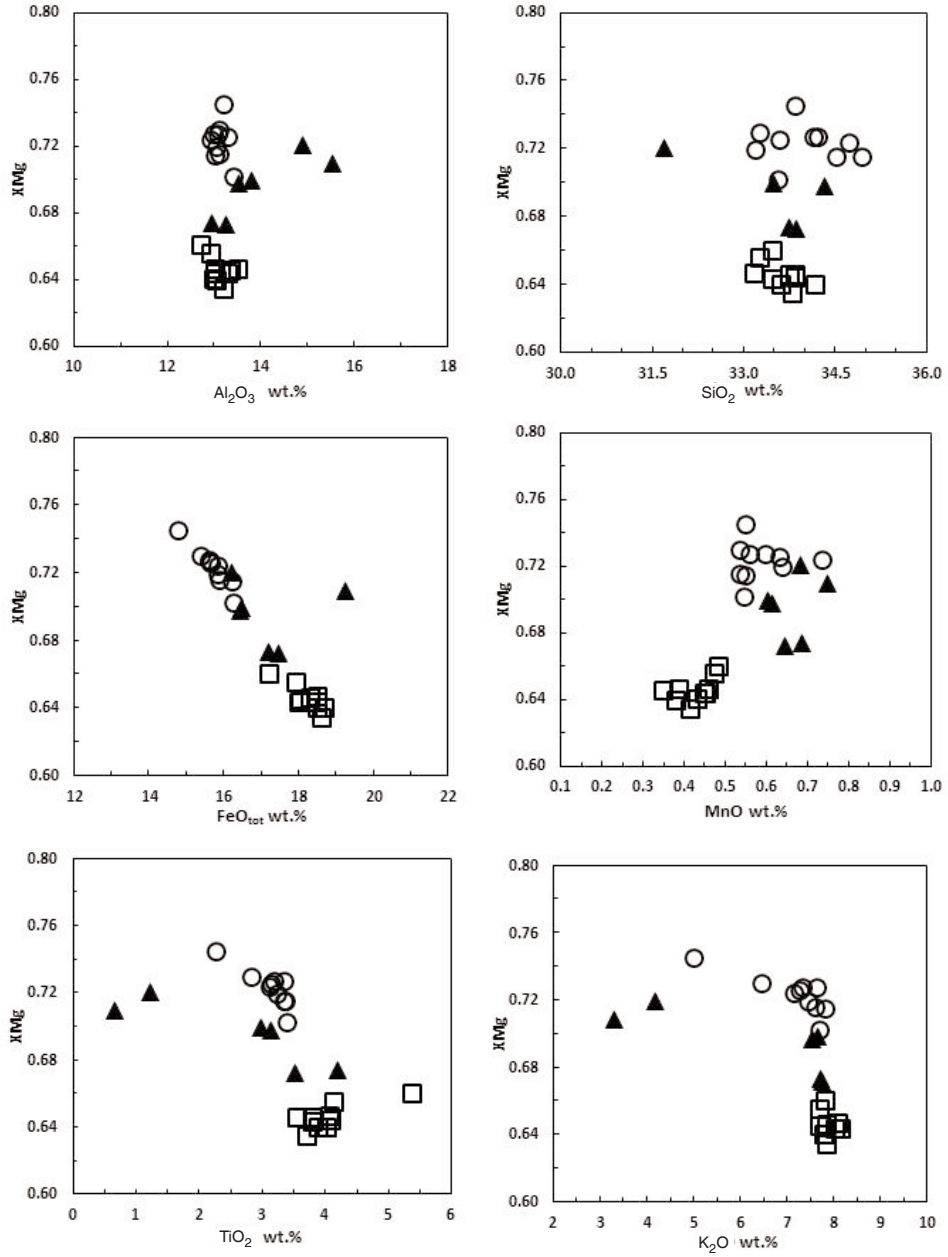

Fig. 7
X_{Mg} vs. wt% SiO_2, Al_2O_3, TiO_2, MnO, Fe_2O_3, and K_2O for magmatic biotite from three rock types of the Shah Jahan Batholith. Each symbol represents one microprobe spot analysis of a biotite crystal (symbols are as in Fig. 6)

oxygen). Based on these criteria, all biotites described here are of primary magmatic origin.

Estimation of fO_2 based on X_{Mg} values of biotite

It is difficult to establish the original oxygen fugacities of parental magmas from the study of granitoids (Wones 1989; Hemly et al. 2004), as magnetite usually becomes Ti-free during slow cooling and ilmenite undergoes one or more stages of oxidation and exsolution (Haggerty 1976). However, the oxidation state of the magma can be estimated using the rock-mineral assemblage and mineral chemistry. Enami et al. (1993) indicated that occurrences of Mg-rich biotite and amphibole in felsic rocks are indicators of relatively oxidized magma. Under such conditions, phlogopitic biotite is normally found with magnetite, titanite, quartz and potassium feldspar (Anthony and Titley 1988; Anthony 2005; Harlov et al. 2006).

Wones (1989) has suggested that the assemblage titanite + magnetite + quartz in granitic rocks permits an estimation of relative oxygen fugacity. Based on the fO_2-T °C diagram of Wones and Eugster (1965) and the X_{Fe} values of biotite, the Shah Jahan granitoids crystallized from highly oxidized magma (Fig. 8). As illustrated in Fig. 8, average oxygen fugacities are approximately $10^{-12.5}$ to $10^{-7.5}$ bars with assumed 700–800 ° C crystallization temperatures at 2 Kbar pressure. This is in good agreement with relatively high oxidizing conditions that were demonstrated by titanite-magnetite-quartz-amphibole-biotite equilibrium (Harlov and Hansen 2005; Harlov et al. 2006).

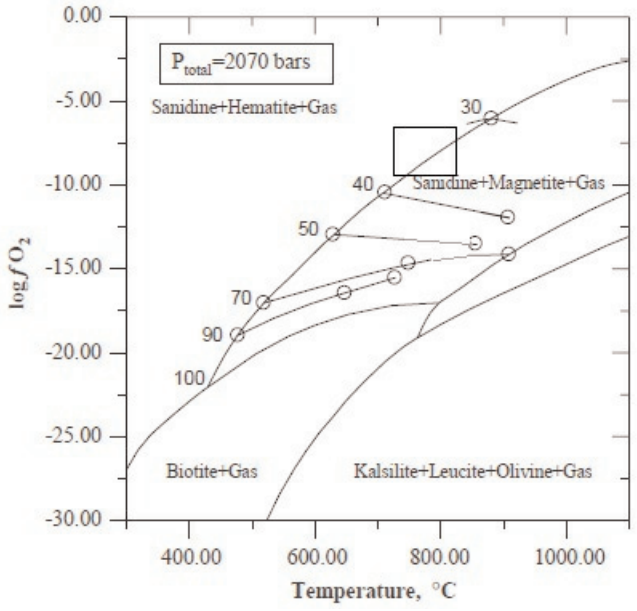

Fig. 8
Field of $\log f_{O2}$-T states of stability for micas on diagram presented by Wones and Eugster (1965), as a function of X_{Fe} values of biotites from the Shah Jahan granitoids (X_{Fe} varies from 0.26 to 0.37; compositional field shown with rectangular box)

Biotite halogen chemistry

Since X_{Mg} of biotite has a considerable effect on F (Munoz and Ludington 1974) and Cl partitioning (Munoz and Swenson 1981), F and Cl wt.% of biotite are plotted versus X_{Mg} values for each of the three intrusives. As illustrated in Fig. 9, these distribution patterns do not show any systematic outline. F contents represent three distinct populations (including 0, ~1–2.2 and ~3.3–4.3 wt.%), whereas Cl demonstrates gradual variations in the range of 0–0.073 wt.% versus different X_{Mg} values of biotite in all rock types.

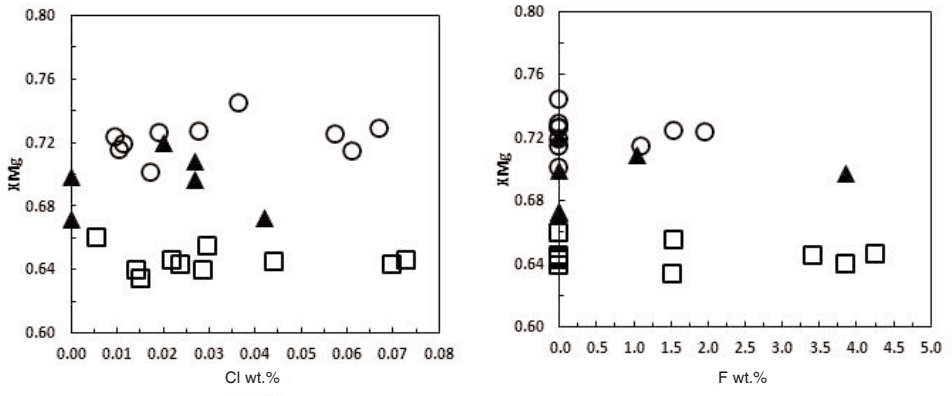

Fig. 9
X_{Mg} vs. F and Cl wt.% for biotite from intrusions in the Shah Jahan batholithic complex (symbols are the same as in Fig. 6)

Biotite with high X_{Mg} incorporates more F in comparison to biotite with lower X_{Mg} values, a crystal-chemical effect referred to as the Fe-F avoidance principle (Munoz 1984). The F content exhibits the highest value in a number of analyzed biotites from Garachilar and Zarlidareh. It decreases below the detection limit value at relatively similar X_{Mg} in more than half of the biotite samples in all three rock types. On the other hand, the Annigh samples that have the highest X_{Mg} value of biotite show moderately low to zero F content. This suggests either that the Fe-F avoidance principle does not apply for these biotites or that the biotite with lower X_{Mg} values has coexisted with a fluid enriched in F. The F value of biotite observed in the Shah Jahan granitoid (1–4 wt.%) has slightly to moderately more F content than the other calc-alkaline intrusions related to Cu-Mo porphyry systems (0.1–1.6 wt.%; Selby and Nesbitt 2000; fig. 3; pp. 84), partly caused by higher X_{Mg} values of studied biotites.

The biotite of Garachilar and Annigh exhibits mean X_{Mg} values of 0.64 and 0.72, respectively, and has typically similar range of Cl content. Biotite with high X_{Mg} values incorporates less Cl than biotite with lower X_{Mg} values; this is an effect referred to as the Mg-Cl avoidance principle (Munoz 1984). The Cl contents of

biotite from Garachilar and Annigh appear to be independent of X_{Mg} values, which are in disagreement with the Mg-Cl avoidance principle. It suggests that either the Mg-Cl crystal chemical effect does not apply to these biotites or biotite with different X_{Mg} values coexists with different Cl-bearing solutions through crystallization. Cl contents of these biotites (~0-0.08 wt.%) are moderately lower than the other mineralized systems (~0.1–0.95 wt.%; Selby and Nesbitt 2000; fig. 3; pp. 84). It can be in part affected by the higher X_{Mg} values in biotite from the Shah Jahan because phlogopite can substitute a maximum of 0.1 wt.% Cl, while the Cl contents of annite can reach more than 1.4 wt.% (Munoz and Swenson 1981).

Estimation of magmatic fluid HF, HCl and H_2O fugacity ratios

In intrusion-related environments, most biotite was formed during crystallization and in part precipitated during hydrothermal alteration of the host intrusives. Since many thermodynamic variables can control the complex chemistry of biotite, its composition is potentially useful for understanding some of the physical and chemical conditions associated with the igneous and hydrothermal events leading to the formation of ore deposits related to an intrusion. Theoretical estimations of F-Cl-OH partitioning between biotite and a melt/or fluid (Zhu and Sverjensky 1991, 1992; Sallet 2000), and equations formulated to determine (H_2O/HF), (H_2O/HCl), and (HF/HCl) fugacity ratios (Munoz 1992) from biotite compositions, allow a more detailed study of the assessment of magmatic/hydrothermal fluids chemistry and their evolution within mineralizing magmatic systems (Yavuz 2003).

Fluorine and chlorine values of biotite were used to determine the (fH$_2$O/fHF), (fH$_2$O/fHCl), and (fHF/fHCl) ratios for magmatic solutions in the studied area. The fugacity ratios were calculated using the equations of Munoz (1992) for magmatic fluids that coexisted with biotite of the studied plutons, based on 1000 °K (~ 727 °C), which is a reasonable crystallization temperature estimated for these intrusions using the hornblende geothermometer (application of hornblende thermometer, equation of Humphreys et al. (2009); authors' unpublished data). Munoz's (1992) equations used for calculating the fugacity ratios are:

$$\text{Log } (fH_2O)/(fHCl)_{fluid} = 1000/T\,(1.15 + 0.55{*}X_{Mg\text{-}(biotite)}) + 0.68 - \log (X_{Cl}/X_{OH})_{biotite}$$

$$\text{Log } (fH_2O)/(fHF)_{fluid} = 1000/T\,(2.37 + 1.1{*}X_{Mg\text{-}(biotite)}) + 0.43 - \log (X_{F}/X_{OH})_{biotite}$$

$$\text{Log } (fHF)/(fHCl)_{fluid} = -1000/T\,(1.22 + 1.65{*}X_{Mg\text{-}(biotite)} + 0.25 + \log (X_{F}/X_{Cl})_{biotite}$$

where T is the temperature of the halogen partitioning between biotite and coexisting fluid in °Kelvin, $X_{Mg\text{-}(biotite)}$ is the Mg/ sum octahedral cations in biotite structural formula, and X_F, X_{Cl}, and X_{OH} are the mole fractions of F, Cl, and OH in the hydroxyl site of the biotite.

The determined fugacity ratios of fluids are plotted in Fig. 10A and B. The magmatic solution from the Garachilar Pluton has similar to slightly higher log (fH$_2$O/fHCl), similar to more positive log (fHF/fHCl), and similar to slightly

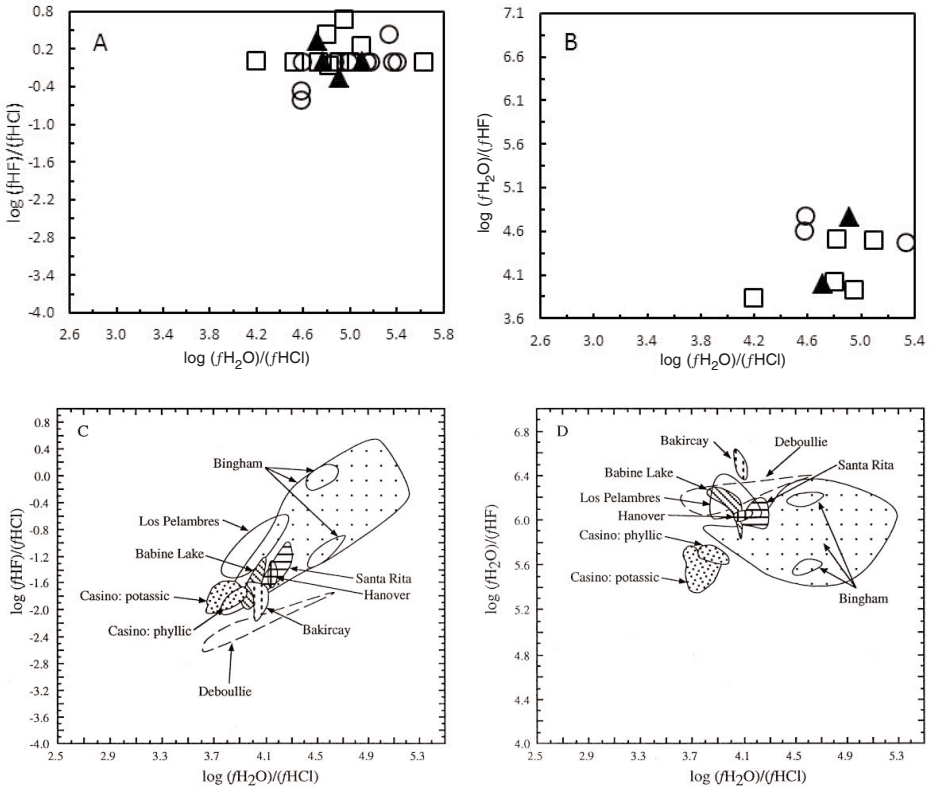

Fig. 10
(A and B) Log (fH_2O/fHF), ($fH_2O/fHCl$), and ($fHF/fHCl$) calculated for magmatic solutions derived from the three intrusions of the Shah Jahan batholithic complex, NW Iran. Fugacity ratios are calculated at 1000 °K for each intrusion (symbols are the same as in Fig. 6). (C and D) Fugacity ratios determined for hydrothermal fluids at some Cu-Mo porphyry-related systems from Selby and Nesbitt (2000)

lower log (fH_2O/fHF) than the solution associated with Annigh. Fugacity ratios calculated for the magmatic fluid derived from Zarlidareh are definitely among the values obtained from the Garachilar and Annigh Plutons. These values vary considerably in each individual sample; nevertheless, the variation is similar for all studied intrusions. It can be related to the combined source of the parental magma and/or similar processes (fractional crystallization/assimilation) contemporaneous with and/or prior to evolution of magmatic-hydrothermal systems that are responsible for intrusion-related mineralization. These differences also indicate that the biotite halogen chemistry is not representative of a single/or constant fluid chemistry.

Our studies indicate that magmatic-hydrothermal fluids that are responsible for mineralization in the Shah Jahan area have similar to slightly higher

($fH_2O/fHCl$), particularly lower (fH_2O/fHF), and similar to a very slightly positive ($fHF/fHCl$) values in comparison to fugacity ratios determined for hydrothermal fluids at some other Cu-Mo porphyry-related systems of Selby and Nesbitt (2000), as shown in Fig. 10C and D. It should be kept in mind that the temperatures and X_{Mg} values used for calculating those fugacity ratios are considerably different; hence, some of the observed diversities were a consequence of these differences. However, the highest similarity in ($fH_2O/fHCl$) and ($fHF/fHCl$) ranges of fluids was observed between the Shah Jahan and the Bingham (Fig. 10).

Discussion and Conclusions

Reviews of ore deposits have identified oxidized and fractionated I-type granitoids as the most favorable host rocks for Cu-Mo-Au porphyry-type deposits (Ishihara 1981; Blevin and Chappell 1992, 1995; Belousova et al. 2002; Ishihara and Chappell 2004; Sillitoe 2003; Vigneresse 2007). The fundamental oxygen fugacity of magma is related to its source materials, which in turn depends on tectonic setting (Carmichael 1991; Ishihara 1977, 2004; Vigneresse 2007). Mineralized I-type granitoids are relatively oxidized (Candela and Bouton 1990; Ishihara 1977, 1981; Ishihara and Chappell 2004; Sillitoe 2003; Vigneresse 2007) and more highly oxidized magmas are commonly related to convergent plate boundaries (Ewart 1979; Loiselle and Wones 1979). The X_{Mg} of biotites is a significant factor and exhibits the indicator characteristics of mineralization features in the three studied intrusions of the Shah Jahan Batholith. Based on occurrences of biotite in equilibrium with titanite, magnetite, quartz, K-feldspar and hornblende, and relatively high X_{Mg} values of biotite, this magmatic system exhibited a high oxidation state. The estimated fO_2 is approximately in the range of $10^{-12.5}$ to$10^{-7.5}$ bars. Presenting such a highly oxidized state for host rocks of biotite illustrates a typical potential for mineralization (especially for Cu-Mo-Au porphyry deposits) in these subduction-related I-type granitoids. On the other hand, according to Uchida et al. (2007), all of our studied intrusions have a characteristic potential for mineralization ($Al_{total} < 3.2$ apfu), in view of the maximum and minimum values of Al_{total} content of biotites, which are 2.82 and 2.23apfu, respectively (Table 1).

Oxidized magmas tend to crystallize biotite of phlogopitic composition, usually with 0.7 or greater mole-fraction of phlogopite (X_{Mg}) (Parry and Jacobs 1975). High Mg values of biotite belong to moderately to highly oxidized magma, and the ferroan samples are related to strongly reduced magma (Anthony 2005). On the other hand, the Mg/Fe ratio of biotite (X_{Mg}) has a considerable effect on F↔OH (Munoz and Ludington 1974) and Cl↔OH partitioning (Munoz and Swenson 1981), where for a given fluid composition and temperature, phlogopite has a considerably higher F and lower Cl content than annite or siderophyllite (Munoz and Ludington 1974). The maximum fluorine contents of these biotites is

slightly higher than some other investigated Cu-Mo porphyry-mineralized intrusions, partly caused by higher X_{Mg} values of the biotite of the Shah Jahan Batholith.

Calc-alkaline granitoids are typically related to water-saturated partial melting of a subducted oceanic crust and the mantle above it, with the possible participation of the lower crust (Wyllie 1984). Their low F contents are thus explained by the nature of the magma source, mantle vs. crustal, and the nature of the melting processes, dry vs. wet (Sallet 2000). F content variations in igneous rocks show two main trends, reflecting the incompatible or compatible behavior of F. Within wet calc-alkaline magmas, F content is decreased as a result of differentiation by crystal fraction of hydrous minerals. Where apatite, amphibole, and biotite are typically early formed phases, F enters the hydroxyl site and behaves as a compatible element. F acts as an incompatible element in dry alkaline high-silica A-type granites where F contents increase as a result of differentiation by crystal fractionation of essentially anhydrous assemblages. This case is observed when biotite, the main OH-bearing phase, is typically a late-stage phase together with characteristic crystallization of fluorite and/or topaz (Kanisawa 1979; Christiansen and Lee 1986). With nearly constant X_{Mg} values, the F content of biotites is erratically decreased to zero for nearly of half of the studied samples that recorded existence of an F-poor solutions (low fHF/fH_2O) in equilibrium with these biotites during crystallization. Detected F trends, in addition to complete absence of fluorite and topaz from studied intrusives and related veins, are consistent with the well-known compatible behavior of F during the differentiation of wet calc-alkaline magmas, where F content decreases as a function of crystal fractionation of minerals such as apatite, amphibole and biotite during magma crystallization (Bailey 1977; Kanisawa 1979; Candela 1986b; Christiansen and Lee 1986; Sallet 2000).

It is recognized that Cl is a particularly significant volatile component in arc systems and its content is high in evolved arc magmas (Wallace 2005). Although Cl can be taken into some phases such as amphibole and biotite, it shows incompatible behavior in melt, particularly within water-saturated systems, and is strongly partitioned into an exsolved vapor phase (Kilinc and Burnham 1972; Webster and Holloway 1988; Webster 1992, 1997). In addition, Cl concentration decreases with increasing X_{Mg} of biotite, which occurs because the large Cl ion can substitute more easily for OH in biotite with Fe^{2+} than Mg^{2+} (Volfinger et al. 1985). Consequently, Cl content increases within a residual melt/fluid as a function of fractional crystallization of oxidized wet granitoidic magma. Apparent Cl-variations in biotites can be related to changes in the major-element composition of biotite (especially Mg/Fe values), the distribution coefficient of Cl between biotite-melt-vapor phases, and/or the melt Cl/OH ratios during the crystallization of magma (Humphreys et al. 2009). The observed trends of Cl in biotites from individual rock samples, in addition to observed residual high salinity magmatic-hydrothermal solutions which are found in fluid inclusions of

cogenetic quartz, reflect that the Cl contents of evolved fluids increase during progressive crystallization of magma.

It seems that initially different contents of F and Cl within subduction-related melt, and their diverse behavior during fractional crystallization of highly oxidized wet calc-alkaline magma, play important roles in chemical composition of evolved magmatic-hydrothermal solutions. Biotite and amphibole, which crystallized under such conditions, normally have high X_{Mg}, allowing more F replacement than Cl in their hydroxyl sites. This can lead progressively to F depletion and Cl enrichment from magmatic-hydrothermal fluid. Such fluids are able to form and concentrate distinctive ranges of metal-bearing complexes which product special types of ore deposits, characteristically porphyry-style Cu-Mo-Au. Subsequently, high-salinity fluid inclusions (halite-saturated) within porphyry-related systems, which entrap from ore-bearing magmatic-hydrothermal solutions, are mainly of chloritic composition (Bodnar and Beane 1980; Roedder 1984; Cline and Bodnar 1994; Ulrich et al. 2001; Zhang et al. 2007). The low F content of fluid inclusions within the hydrothermally-altered zones of porphyry Cu deposits indicates that the fluids derived from magma are not F-rich (Sallet 2000).

High fO_2 and calculated fH_2O/fHF and $fH_2O/fHCl$ fields for the Shah Jahan plutons are in good agreement with essential oxidized conditions of Cu-Mo-Au-mineralized source magma (Candela 1986a; Candela and Bouton 1990; Meinert 1995; Christiansen and Keith 1996; Newberry 1998; Aksyuk 2000; Lentz and Suzuki 2000; Anthony 2005), and with the required roles of F and Cl in participating in the formation of metal-bearing magmatic-hydrothermal fluids (Marakushev 1979; Candela and Holland 1984, 1986; Eugster 1985; Candela 1986b; Keppler and Wyllie 1991; Candela and Piccoli 1995; Wood and Samson 1998; Aksyuk 2000).

Acknowledgements

The authors thank the exploration department of National Iranian Copper Industries Company (NICICO), for funding this investigation. The support of Mohammad Kargar and Dr. Hassan Koshrou, Administrators of Exploration and Engineering development of NICICO, were a prerequisite for initiation and completion of the research. We thank the EMPA Center at the Department of Applied Geosciences and Geophysics, Montan University of Leoben, Austria, and the staff for Dr. mont A.M. Azimzadeh for assistance in analytical procedures and BSE imaging.

References

Abdel-Rahman, A-F.M. 1994: Nature of biotites from alkaline, calc-alkaline and peraluminous magmas. – Journal of Petrology, 35/2, pp. 525–541.

Aksyuk, A.M. 2000: Estimation of Fluorine concentrations in fluids of mineralized skarns systems. – Economic Geology, 95, pp. 1339–1347.

Alavi, M. 1991: Tectonic Map of the Middle East, 1: 5000000. – Geological Survey of Iran.

Anthony, E.Y. 2005: Source regions of granites and their links to tectonic environment: examples from the western United States. – Lithos, 80, pp. 61–74.

Anthony, E.Y., S.R. Titley 1988: Progressive mixing of isotopic reservoirs during magma genesis at the Sierrita porphyry copper deposit: inverse solutions. – Geochimica et Cosmochimica Acta, 52, pp. 2235– 2249.

Bailey, J.C. 1977: Fluorine in granitic rocks and melts: a review. – Chemical Geology, 19, pp. 1–42.

Beane, R.E. 1974: Biotite stability in the porphyry copper environment. – Economic Geology, 69, pp. 241–256.

Belousova, E.A., W.L. Griffin, S.Y. O'Reilly, N.I. Fisher 2002: Apatite as an indicator mineral exploration: trace-element compositions and their relationship to host rock type. – Journal of Geochemical Exploration, 76, pp. 45–69.

Blevin, P.L., B.W. Chappell 1992: The role of magma sources, oxidation states, and fractionation in determining the granite metallogeny of eastern Australia. – Transactions of the Royal Society of Edinburgh. Earth Sciences, 83, pp. 305–316.

Blevin, P.L., B.W. Chappell 1995: Chemistry, origin and evolution of mineralized granites in the Lachlan Fold Belt, Australia: the metallogeny of I- and S-type granites. – Economic Geology, 90, pp. 1604–1619.

Bodnar, R.J., R.E. Beane 1980: Temporal and spatial variations in hydrothermal fluid characteristics during vein filling in preore cover overlying deeply buried porphyry copper-type mineralization at Red Mountain, Arizona. – Economic Geology, 75, pp. 876–893.

Bowman, J.R., W.T. Parry, W.P. Kropp, S.A. Kruer 1987: Chemical and isotopic evolution of hydrothermal solutions at Bingham. Utah. – Economic Geology, 82, pp. 395–428.

Candela, P.A. 1986a: The evolution of aqueous vapor from silicate melts: Effect of oxygen fugacity. – Geochimica et Cosmochimica Acta, 50, pp. 1205–1211.

Candela, P.A. 1986b: Toward a thermodynamic model for the halogens in magmatic systems: an application to melt-vapor-apatite equilibrium. – Chemical Geology, 57, pp. 289–301.

Candela, P.A., S.L. Bouton 1990: The influence of oxygen fugacity on tungsten and molybdenum partitioning between silicate melts and ilmenite. – Economic Geology, 85, pp. 633–640.

Candela, P.A., H.D. Holland 1984: The partitioning of copper and molybdenum between silicate melts and aqueous fluids. – Geochimica et Cosmochimica Acta, 48, pp. 373–380.

Candela, P.A., H.D. Holland 1986: A mass transfer model for copper and molybdenum in magmatic hydrothermal systems: The origin of porphyry-type ore deposits. – Economic Geology, 81, pp. 1–19.

Candela, P.A., P.M. Piccoli 1995: Model ore-metal partitioning from melt into vapor and vapor/brine mixtures. – Mineralogical Association of Canada Short Course, 23, pp. 101–127.

Carmichael, I.S.E. 1991: The redox state of basic and silicic magmas: a reflection of their source region. – Contributions to Mineralogy and Petrology, 106, pp. 129–141.

Christiansen, E.H., D. Lee 1986: Fluorine and chlorine in granitoids from the Basin and Range Province, Western United States. – Economic Geology, 81, pp. 1484–1494.

Christiansen, E.H., J.D. Keith 1996: Trace element systematics in silisic magmas: A metallogenic perspective. – Geological Association of Canada Short Course Notes 12, pp. 115–151.

Cline, J.S., R.J. Bodnar 1994: Direct evolution of brine from a crystallizing silicic melt at the Questa, New Mexico, molybdenum deposit. – Economic Geology, 89, pp. 1780–1802.

Coulson, I.M., G.M. Dipple, M. Raudsepp 2001: Evolution of HF and HCl activity in magmatic volatiles of the gold-mineralized Emerald Lake pluton, Yukon Territory, Canada. – Mineralium Deposita, 36, pp. 594–606.

Deer, W.A., R.A. Howie, J. Zussman 1991: An introduction to the Rock-Forming Minerals. – Longman Scientific and Technical, United States, Seventeenth impression, 528 p.

Deer, W.A., R.A. Howie, J. Zussman 1992: An introduction to the Rock-Forming Minerals, 2nd edition. – Longman Scientific and Technical, 696 p.

Enami, M., K. Suzuki, J.G. Liou, D.K. Bird 1993: Al–Fe^{3+} and F–OH substitutions in titanite and constrains on their P–T dependence. – European Journal of Mineralogy, 5, pp. 231–291.

Eugster, H.P. 1985: Granites and hydrothermal ore deposits: A geochemical framework. – Mineralogical Magazine, 49, pp. 7–23.

Ewart, A. 1979: A review of the mineralogy and chemistry of Tertiary-recent dacitic, latitic, rhyolitic and related salic volcanic rocks. – In: Fred, B. (Ed.): Trondhjemites, dacites, and related rocks. Springer Verlag, Berlin, pp.12–101.

Farmer, G.L., A.L. Boettcher 1981: Petrologic and crystal-chemical significance of some deep-seated phlogopites. – American Mineralogists, 66, pp. 1154–1163.

Haggerty, S.E. 1976: Opaque mineral oxides in terrestrial igneous rocks. – Mineralogical Society of American Short Course Notes, 3, pp. 101–300.

Harlov, D., P. Tropper, W. Seifert, T. Nijland, H.J. Forster 2006: Formation of Al-rich titanite ($CaTiSiO_4OH$–$CaAlSiO_4OH$) reaction rims on ilmenite in metamorphic rocks as a function of f_{H2O} and f_{O2}. – Lithos, 88, pp. 72–84.

Harlov, D.E., E.C. Hansen 2005: Oxide and sulphide isograds along a late Archean, deep-crustal profile in Tamil Nadu, South India. – J. Met. Geol., 23, pp. 241–259.

Hemly, H.M., A.F. Ahmed, M.M. El Mahallawi, S.M. Ali 2004: Pressure, temperature and oxygen fugacity conditions of calc-alkaline granitoids, Eastern Egypt, and tectonic implications. – Journal of African Earth Sciences, 38, pp. 255–268.

Humphreys, M.C.S, M. Edmonds, T. Christopher, V. Hards 2009: Chlorine variations in the magma of Soufriere Hills Volcano, Montserrat: Insights from Cl in hornblende and melt inclusions. – Geochimica et Cosmochimica Acta, 73, pp. 5693–5708.

Ishihara, S. 1977: The magnetite series and ilmenite series granite rocks. – Mining Geology, 27, pp. 293–305.

Ishihara, S. 1981: The granitoid series and mineralization. – Economic Geology, 75th Anniversary, pp. 458–484.

Ishihara, S. 2004: The redox state of granitoids relative to tectonic setting and earth history: the magnetite-ilmenite series 30 years later. Transactions of the Royal Society of Edinburgh. – Earth Sciences, 95, pp. 23–33.

Ishihara, S., B.W. Chappell 2004: A special issue of granites and metallogeny: the Ishihara volume. – Resource Geology, 54, pp. 213–382.

Jacobs, D.C., W.T. Parry 1979: Geochemistry of biotite in the Santa Rita porphyry copper deposit, New Mexico. – Economic Geology, 74, pp. 860–887.

Kanisawa, S. 1979: Content and behavior of fluorine in granitic rocks, Kitami Mountains, Northeast Japan. – Chemical Geology, 24, pp. 57–67.

Keppler, H., P.J. Wyllie 1991: Partitioning of Cu, Sn, Mo, W, U, and Th between melt and aqueous fluid in the systems haplogranite-H_2O-HCl and haplogranite-H_2O-HF. – Contributions to Mineralogy and Petrology, 109, pp. 139–150.

Kilinc, I.A., C.W. Burnham. 1972: Partitioning of chloride between a silicate melt and coexisting aqueous phase from 2 to 8 Kbar and 800°C. – European Journal of Mineralogy, 6, pp. 913–923.

Lentz, D.R., K. Suzuki 2000: A low F pegmatite related Mo skarn from the southwestern Grenvile Province, Ontario, Canada: Phase equilibria and petrogenetic implications. – Economic Geology, 95, pp. 1319–1337.

Loferski, P.J., R.A. Ayuso 1995: Petrology and mineral chemistry of the composite Deboullie pluton, northern Maine, USA: Implication for the genesis of Cu-Mo mineralization. – Chemical Geology, 123, pp. 89–105.

Loiselle, M.C., D.R. Wones 1979: Characteristics and origin of anorogenic granites. – Geological society of America, Abstracts with Program, 7, p. 468.

Marakushev, A.A. 1979: Petrogenesis and ore-formation (geochemical aspects): Moscow. – Nauka, p. 264. (In Russian.)

Meinert, L.D. 1995: Compositional variation of igneous rocks associated with skarn deposits-chemical evidence for a genetic connection between petrogenesis and mineralization. – Mineralogical Association of Canada Short Course Handbook, 23, pp. 401–418.

Mokhtari, M.A.A. 2009: Petrology, geochemistry and petrogenesis of Qaradagh Batholith (East of Syahrood, Eastern Azerbaijan) and Related skarns, with considering mineralization. – Ph.D. thesis, Tarbiat Modares University, Iran, 317 p. (In Persian.)

Munoz, J.L. 1984: F-OH and Cl-OH exchange in micas with applications to hydrothermal ore deposits. 317 p. In: Bailey, S.W. (Ed.): Micas. Rev. Mineral., 13, pp. 469–494.

Munoz, J.L. 1990: F and Cl contents of hydrothermal biotites: a re-evaluation. – Geological Society of America, Abstract. Programs, 22, A135.

Munoz, J.L. 1992: Calculation of HF and HCl fugacities from biotite compositions: revised equations. – Geological Society of America, Abstract. Programs, 24, A221.

Munoz, J.L., S.D. Ludington 1974: Fluoride-hydroxyl exchange in biotite. – Am. Journal of Science, 274, pp. 396–413.

Munoz, J.L., A. Swenson 1981: Chloride-hydroxyl exchange in biotite and estimation of relative HCl–HF activities in hydrothermal fluids. – Economic Geology, 76, pp. 2212–2221.

Nachit, H., N. Razafimahefa, J.M. Stussi, J.P. Carron 1985: Composition chimique des biotites et typologie magmatique des granitoides. – Comptes rendus de l'Académie des sciences, 301/11, pp. 813–818.

Nachit, H., I. Abderrahmane, E.H. Abia, M. Ben Ohoud 2005: Discrimination between primary magmatic biotites, reequilibrated biotites and neoformed biotites. – C. R. Geoscience, 337, pp. 1415–1420.

Newberry, R.J. 1998: W- and Sn-skarn deposits: A 1998 status report. – Mineralogical Association of Canada Short Course Handbook, 26, pp. 289–335.

Parry, W.T., D.C. Jacobs 1975: Fluorine and chlorine in biotite from Basin and Range plutons. – Economic Geology, 70, pp. 554–558.

Rieder, M. 2001: Mineral nomenclature in the mica group: the promise and the reality. – European Journal of Mineralogy, 13/6, pp. 1009–1012.

Rieder, M., G. Cavazzini, Y.S. D`Yakonov, V.A. Frank-Kamentskii, G. Gottardi, S. Guggenheim, P.V. Koval, G. Müller, A.M.R. Neiva, E.W. Radoslovich, J-L. Robert, F.P. Sassi, H. Takeda, Z. Weiss, D.R. Wones 1998: Nomenclature of the micas. – The Canadian Mineralogist, 36, pp. 41–48.

Roedder, E. 1984. Fluid Inclusions. – In: Ribbe, P.H. (Ed.): Reviews in Mineralogy, 12. 636 p.

Sallet, R. 2000: Fluorine as a tool in the petrogenesis of quartz-bearing magmatic associations: applications of an improved F-OH biotite-apatite thermometer grid. – Lithos, 50, pp. 241–253.

Selby, D., B.E. Nesbitt 2000: Chemical composition of biotite from the Casino porphyry Cu-Au-Mo mineralization, Yukon, Canada: evaluation of magmatic and hydrothermal fluid chemistry. – Chemical Geology, 171, pp. 77–93.

Schmidt, M.W. 1992: Amphibole composition in tonalite as a function of pressure: an experimental calibration of the Al-in-hornblende barometer. – Contribution to the Mineralogy and Petrology, 110, pp. 304–310.

Sillitoe, R.H. 2003: Iron oxide-copper-gold deposits: an Andean view. – Mineralium Deposita, 38, pp. 787–812.

Uchida, E., S. Endo, M. Makino 2007: Relationship between solidification depth of granitic rocks and formation of hydrothermal ore deposits. – Resource Geology, 57, pp. 47–56.

Ulrich, T., D. Gunther, C.A. Heinrich 2001: The evolution of a porphyry Cu-Au deposit, based on LA-ICP-MS analysis of fluid inclusions: Bajo de la Alumbrera, Argentinafs. – Economic Geology, 96, pp. 1743–1774.

van Middelaar, W.T., J.D. Keith 1990: Mica chemistry as an indicator of oxygen and halogen fugacities in the CanTung and other W-related granitoids in the North American Cordillera. – Geological Society of America. Special Paper, 246, pp. 205–220.

Vigneresse, J.L. 2007: The role of discontinuous magma inputs in felsic magma and ore generation. – Ore Geology Reviews, 30, pp. 181–216.

Volfinger, M., J.-L.Robert, D. Vielzeuf, A.M.R. Neiva 1985: Structural control of the chlorine content of OH-bearing silicates (mica and amphiboles). – Geochimica Cosmochimica Acta, 49, pp. 37–48.

Wallace, P.J. 2005: Volatiles in subduction zone magmas: concentrations and fluxes based on melt inclusion and volcanic gas data. – Journal of Volcanology and Geothermal Research, 140, pp. 217–240.

Webster, J.D. 1992: Fluid-melt interactions involving Cl-rich granites: experimental study from 2 to 8 kbar. – Geochimica Cosmochimica Acta, 56, pp. 659–678.

Webster, J.D. 1997: Chloride solubility in felsic melts and the role of chloride in magmatic degassing. – Journal of Petrology, 38, pp. 1793–1807.

Webster, J.D., J.R. Holloway 1988: Experimental constraints on the partitioning of Cl between topaz rhyolite melt and H_2O and H_2O+CO_2 fluids: new implications for granitic differentiation and ore deposition. – Geochimica Cosmochimica Acta, 52 pp. 2091–2105.

Wyllie, J. 1984: Constrains imposed by experimental petrology on possible and impossible magma sources and products. – Philosophical Transactions of the Royal Society of London, A, 310, pp. 439–456.

Wones, D.R. 1972: Stability of biotite: a reply. – American Mineralogist, 57/1–2, pp. 316–317.

Wones, D.R. 1981: Mafic silicates as indicators of intensive variables in granitic magmas. – Mining Geology (Japan), 31, pp. 191–212.

Wones, D.R. 1989: Significance of the assemblage titanite+ magnetite+quartz in granitic rocks. – American Mineralogist, 74, pp. 744–749.

Wones, D.R., H.P. Eugster 1965: Stability of biotite: experiment, theory, and application. – American Mineralogist, 50, pp. 1228–1272.

Wood, S.A., I.M. Samson 1998: Solubility of ore minerals and complexion of ore metals in hydrothermal solutions. – Reviews in Economic Geology, 10, pp. 33–80.

Yavuz, F. 2003: Evaluating micas in petrologic and metallogenic aspect: Part II – Applications using the computer program Mica+. – Computer Geosciences, 29, pp. 1215–1228.

Zakeri, L., A.M. Azimzadeh, F. Malekgasemi 2010: Geochemistry of biotites in the Shah Jahan Cu-Mo-Au mineralized batholith (NW Iran) and its petrological and metallogenic implications. – PANGEO 2010 Abstracts, Journal of Alpine Geology, 52, pp. 260–261.

Zhang, D., G. Xu, W. Zhang, S.D. Golding 2007: High salinity fluid inclusions in the Yinshan polymetallic deposit from the Le-De metallogenic belt in Jiangxi Province, China: Their origin and implications for ore genesis. – Ore Geology Reviews, 31, pp. 247–260.

Zhu, C., D.A. Sverjensky 1991: Partitioning of F-Cl-OH between minerals and hydrothermal fluids. – Geochimica Cosmochimica Acta, 55, pp. 1837–1858.

Zhu, C., D.A. Sverjensky 1992: F-Cl-OH partitioning between biotite and apatite. – Geochimica Cosmochimica Acta, 56, pp. 3435–3467.